

Using windscreens to improve the efficiency of noise barriers in wind: finite-difference time-domain simulations

PACS REFERENCE: 43.28.Js, 43.28.Gq, 43.50.Gf

Van Renterghem Timothy; Botteldooren Dick
University of Ghent, Department of Information technology
Sint-Pietersnieuwstraat 41
9000 Gent
Belgium
+32 (0)9 267 35 94
+32 (0)9 267 35 99
E-mail: Timothy.Van.Renterghem@intec.rug.ac.be; Dick.Botteldooren@intec.rug.ac.be

ABSTRACT The efficiency of noise barriers in wind is strongly reduced in the downwind direction due to screen-induced refraction of sound. The use of windscreens to cope with this problem is proposed. In a wind tunnel experiment, a scale model of a traffic situation was set up. Synthetic windbreaks were efficient to optimize barrier configurations. Same trends were observed during a field experiment along a highway, now using trees as windscreens. These experimental results are now compared to finite-difference time-domain simulations, taking into account high-detailed CFD calculations of the flow near the barriers. Noise barriers on either side of the road are of particular interest.

INTRODUCTION

Wind flowing over a noise barrier will reduce its acoustic efficiency for receivers downwind: large gradients in the wind speed and as a consequence in the effective sound speed appear near the barrier. This screen-induced (downward) refraction reduces significantly the shadow zone behind a noise barrier. This is a well-known and intensively investigated problem [e.g. 1-2]. However, very few solutions to this problem are proposed.

In a wind tunnel study at scale [3], the effect of windscreens on noise barrier performance was investigated. Different configurations of noise barriers were tested, in combination with synthetic woven windscreens, made of polyester. These windscreens were used as a scale model for trees and their porosity range is representative for the porosity of the canopy of trees. Two wind speeds were tested (6.4 m/s and 11 m/s, measured above the boundary layer). The efficiency of the windscreens was measured as a function of distance behind the noise barrier. This paper focusses on the effect of windscreens on double noise barrier configurations, i.e. a noise barrier on either side of a line source. Frequencies ranging from 10 kHz till 20 kHz were used in the experiment. Taking into account a scaling factor of 20, the wind tunnel experiment was performed for the most important frequency range of the traffic noise spectrum.

The finite-difference time-domain (FDTD) method is used to simulate the effect of the windscreens on the noise barrier performance in wind. FDTD is an interesting simulation technique for the study of wave phenomena [e.g. 4]. The relative ease to implement and the clarity of the scheme are important advantages. A finite-difference time-domain formulation for the simulation of sound propagation in a non-uniform, rotational background flow is developed. No restrictions to the flow field are imposed. This is an improvement upon BEM/FEM techniques found in literature where background flow is restricted to uniform flow or parallel flow.

FINITE-DIFFERENCE TIME-DOMAIN SIMULATIONS IN BACKGROUND FLOW

Mathematical Model

The effect of the movement of the fluidum is treated as a perturbation of the acoustic equations. Coupling between fluid flow and acoustics is limited in the present model. Sound generation is not treated, and the acoustic waves will not influence the flow profile.

The basic fluidum equations i.e. the conservation of impulse and the conservation of mass are used as a starting point to derive the equations for sound propagation in background flow. Pressure, fluid density and fluid velocity can be split into an acoustic part and a part attributed to the background flow.

Some assumptions are made concerning the background flow and the acoustics. The background flow is approximated as an incompressible and time-invariant flow. Isothermic flow is assumed. Only linear acoustics are considered. Source terms i.e. all terms that do not contain the acoustic quantities are neglected in the equations. The acoustic compression is assumed to be adiabatic, this means that a linear pressure-density relation can be used.

Some important measures have to be taken to ensure stable simulations. During the derivation of the velocity equation, a kinetic energy conservation form has to be used. Terms containing the rotor of the acoustic velocity are small in comparison to other terms in the equations. The introduction of this condition is however important and is made explicit to prevent the acoustic part of the equations to evolve containing parts of the fluid flow during simulations.

Taking into account the above mentioned assumptions, the following equations are obtained:

$$\frac{\partial \mathbf{v}}{\partial t} - \mathbf{v} \times (\tilde{\mathbf{N}} \times \mathbf{v}_0) + \frac{1}{\rho_0} \tilde{\mathbf{N}} p + \tilde{\mathbf{N}} [\mathbf{v} \cdot \mathbf{v}_0] = 0 \quad (1)$$

$$\frac{\partial p}{\partial t} + c^2 \rho_0 \tilde{\mathbf{N}} \cdot \mathbf{v} + \mathbf{v}_0 \cdot \tilde{\mathbf{N}} p = 0 \quad (2)$$

where v is the acoustic velocity, p is the acoustic pressure, v_0 is the background fluid flow velocity (obtained from a computational fluid dynamic simulation (CFD)), ρ_0 is the ambient mass density, and c is the speed of sound.

Finite-difference Time-domain Model

The use of a staggered grid has shown to have particular advantages for acoustic simulations [5]. In a Cartesian grid, the acoustic pressure is determined in the centre of the (volume of the) FDTD cells at sampled times t . The acoustic velocity is discretised on the surfaces that border each cell and are calculated at intermediate times $(t+0.5) dt$.

The discretisation of equations (1) and (2) to an efficient time stepping formalism is not straightforward. In between two time steps, a prediction step is used neglecting background flow. This results in a numerical efficient calculation scheme, since the inversion of a band matrix is avoided. Such an approximation is accurate as long as the Mach number is not too high. Wind velocities encountered in outdoor sound propagation will not be influenced by this approximation. However, the problem of accuracy for high Mach numbers can always be bypassed using more simulation cells relative to the wavelengths of the sound under investigation.

Adaptations For Outdoor Sound Propagation

Ground

A non-locally reacting ground is used for the simulations. Natural soils can often be modeled as a porous medium. Following equations describe sound propagation in a porous media with a rigid frame. Only the air in between the soil particles is the propagation medium. In this model, the ground is described by three parameters: flow resistivity (R), porosity (β) and the structure factor (k_s) [6]

$$\bar{\nabla} \cdot p + \rho' \frac{\partial \bar{v}}{\partial t} + R \bar{v} = 0 \quad (3)$$

$$\frac{\partial p}{\partial t} + \rho' c'^2 \bar{\nabla} \cdot \bar{v} = 0 \quad (4)$$

where

$$\rho' = \frac{\rho_0 k_s}{\phi}, \quad c' = \frac{c_0}{\sqrt{k_s}} \quad (5),(6)$$

Free sound propagation in air (in absence of flow) can be seen as an extension of the previous equations when using

$$k_s = 1, \mathbf{j} = 1, R = 0 \quad (7),(8),(9)$$

The normalized complex impedance of the ground yields:

$$Z = \sqrt{\frac{R}{\rho\omega\phi} i + \frac{k_s}{\phi^2}}. \quad (10)$$

The FDTD discretisation of these equations introduces no particular difficulties.

Perfectly absorbing boundary conditions

In outdoor sound propagation applications, the simulation domain is usually not physically bounded. The unlimited propagation region has to be truncated to limit the calculation domain. To avoid that this truncation will influence the acoustic calculations, one needs to apply "perfectly absorbing boundary" (PAB) conditions at the border of the simulation grid. Very good PABs e.g. Perfectly Matched Layers (PML) [7] were developed in the field of electromagnetics for the FDTD method. However, these boundary conditions have not been extended to the case of sound propagation in background flow.

When applying a PML or a Berenger boundary condition, the simulation domain has to be extended with a number of cells, in which a non-physical propagation occurs. The acoustic equations are extended with artificial damping for the calculation of the propagation in this Berenger layer. The derivation of the PML equations is based on the acoustic equations for a uniform background flow, normal (=direction \mathbf{a}) to the interface between the PML layer and propagating medium.

$$\frac{\partial p_{\perp}}{\partial t} + c^2 \rho_0 \frac{\partial v_{\alpha}}{\partial \alpha} + v_{0\alpha} \frac{\partial p_{\perp}}{\partial \alpha} + \kappa_{1,\perp} p_{\perp} = 0 \quad (11)$$

$$\frac{\partial p_{\parallel}}{\partial t} + c^2 \rho_0 \sum_{\gamma \neq \alpha} \frac{\partial v_{\gamma}}{\partial \gamma} + v_{0\alpha} \frac{\partial p_{\parallel}}{\partial \alpha} + \kappa_{1,\parallel} p_{\parallel} = 0 \quad (12)$$

$$p_{\perp} + p_{\parallel} = p \quad (13)$$

$$\rho_0 \left[\frac{\partial v_{\alpha}}{\partial t} + v_{0\alpha} \frac{\partial v_{\alpha}}{\partial \alpha} \right] + \frac{\partial p}{\partial \alpha} + \kappa_{2,\perp} v_{\alpha} = 0 \quad (14)$$

$$\rho_0 \left[\frac{\partial v_{\beta}}{\partial t} + v_{0\alpha} \frac{\partial v_{\beta}}{\partial \alpha} \right] + \frac{\partial p}{\partial \beta} + \kappa_{2,\parallel} v_{\beta} = 0, \quad \beta \neq \alpha \quad (15)$$

Splitting the acoustic pressure in an artificial component normal to the Berenger-interface (p_{\perp}), and a component parallel to the interface (p_{\parallel}) results in an additional degree of freedom. This split-field approach makes it possible to fully transmit plane waves at all angles of incidence to the Berenger layer. Artificial damping coefficients κ were introduced in the previous equations. If the following conditions are satisfied, both media are perfectly matched:

$$\kappa_{2,\parallel} = \kappa_{1,\parallel} = 0, \quad \kappa_{1,\perp} = \frac{\kappa_{2,\perp}}{\rho_0} \quad (16),(17)$$

Some reflection will however occur in the discrete FDTD grid, since the abrupt change in damping may lead to some reflection. To reduce this discontinuity at the interface, Berenger [8] proposed to scale the material parameters along the normal axis on the interface, according to

$$\kappa_{1,\perp}(x) = \kappa_{1,\perp,MAX} \left(\frac{x}{d_{PML}} \right)^m, \quad (18)$$

where x is the depth inside the layer normal to the interface and d_{PML} is the total thickness of the PML. It is found that the parameter m is preferably chosen between 3 and 4 [8]

In most practical situations, e.g. in ducts and for outdoor sound propagation in wind, non-uniform flow occur only in small areas on borders. However, using the uniform flow PML equations in a parallel flow will still be an important improvement relative to e.g. first order approximation PABs.

SIMULATION RESULTS

In Figure 1, an overview is given of the acoustic grid (FDTD) and the grid used for flow calculations (CFD). The windscreens are modelled with the porous baffle option of the CFD package STAR-CD [9]. Measurements in the velocity range of interest have indicated that the pressure drop over the windscreens in our test set-up can be described with high correlation by the following quadratic equation:

$$\Delta p = av^2 + bv \quad (19)$$

with $a = 5.040 \text{ Pa s}^2/\text{m}^2$ and $b = 0.092 \text{ Pa s/m}$ [10].

For different noise barrier and windscreen configurations, wind velocity is measured in the wind tunnel during the experiment. The best correspondence between wind velocity calculations and experimental data is obtained using a steady state, k- ϵ turbulence flow model. The parameters of this turbulence model were optimised. A logarithmic wind speed profile is used as a inflow boundary condition.

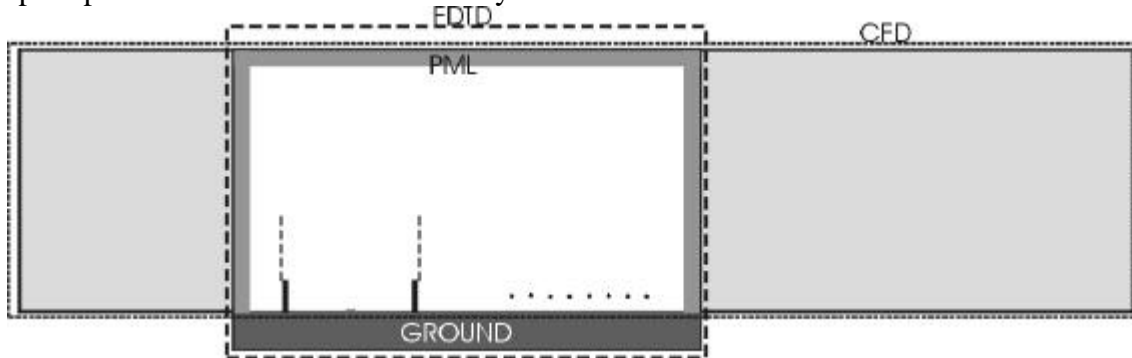


Figure 1. Overview of the CFD grid and FDTD grid, with indication of the PML layers and the region where the ground propagation equations are applied.

FDTD simulations, taking into account high-detailed flow calculations in the vicinity of the noise barriers were performed. In a 2D-grid, a line source is easily simulated. Perfectly matched layers are used to border the calculation grid. An attenuation of the reflection on these layers by more than 100 dB can be obtained when using appropriate values for the damping coefficients. The windscreens were not acoustically modeled, since their effect in the scale experiment on the frequencies considered was small. Only their effect on the flow was taken into account in the acoustic simulations. In Figure 2, an overview of the different configurations of windscreens for the double noise barrier set-up is given. In Figure 3, one finds the results of the CFD simulation (magnitude of the horizontal flow velocity) in the FDTD region for configuration C.



Figure 2. Overview of the double noise barrier configurations under investigation

A comparison is made between the measured and simulated results of the net efficiency of the windscreens. The net efficiency is defined as the difference between the sound pressure level of a noise barrier configuration in absence of windscreens, and the sound pressure level for the

same barrier configuration in combination with windscreens, measured at the same place and for the same wind speed above the boundary layer.

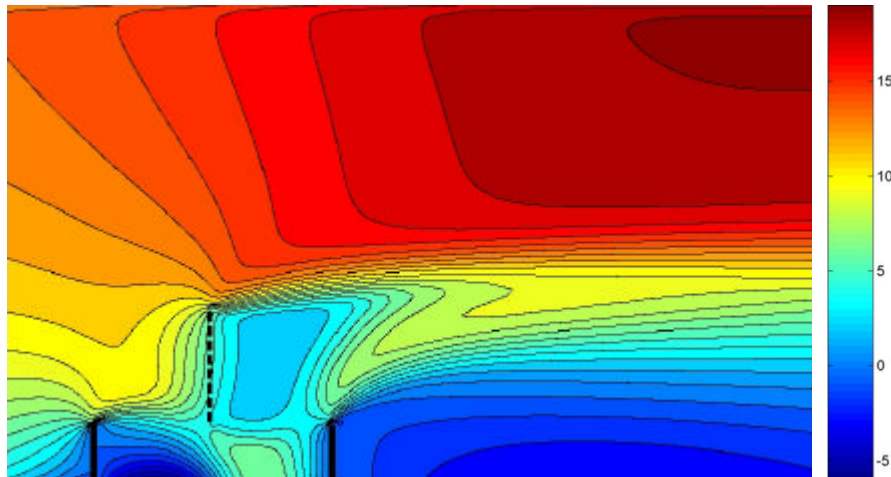


Figure 5. Horizontal flow velocity (m/s) for configuration C in the FDTD region. The incident horizontal flow velocity above the boundary layer is 11 m/s.

The results of this comparison can be found in Figures 3 and 4, for wind speeds of 6.4 m/s and 11 m/s above the boundary layer respectively. Net efficiency (dLp) with increasing distance behind the downwind noise barrier is shown.

In general, good agreement is obtained and discrepancies lie well within the experimental error. A good (CFD) modeling of the gradients in the vicinity of the barriers explains already a great part of the effect of the windscreens. However, the high degree of turbulence in the air flow in the wind tunnel is not taken into account in the acoustic simulations. Configurations A and C may be more sensitive to turbulent effects, since shielding of the wind is lower in these cases.

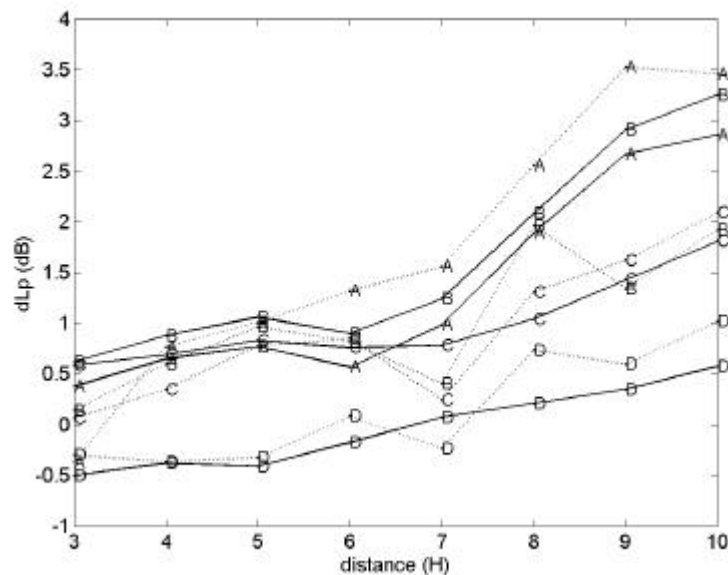


Figure 3. Comparison of the net efficiency of the windscreens between wind tunnel experiment (dashed lines) and FDTD simulations (full lines), with increasing distance behind the downwind noise barrier. The wind speed above the boundary layer is **6.4 m/s**. The distances are expressed in noise barrier heights.

Very good agreement is found for configuration D and B. At larger distances behind the downwind noise barrier and for a wind velocity of 6.4 m/s, the decrease in dLp for configuration B is probably due to experimental errors.

The efficiency of the windscreens in configuration A seems to be better than for configuration B in the experiment. Based on the simulations, one comes to another conclusion. However, differences between the simulated configurations are small.

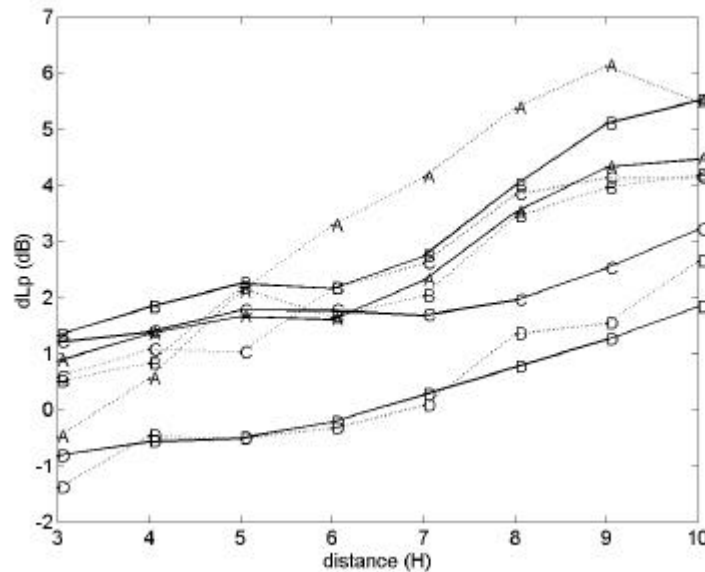


Figure 4. Comparison of the net efficiency of the windscreens between wind tunnel experiment (dashed lines) and FDTD simulations (full lines), with increasing distance behind the downwind noise barrier. The wind speed above the boundary layer is **11 m/s**. The distances are expressed in noise barrier heights.

CONCLUSIONS

A finite-difference time-domain model was developed to study sound propagation in a non-uniform, rotational background flow. Adaptations were made to use this model in outdoor situations. Perfectly matched layers in uniform flow were introduced and border the calculation domain. A non-locally reacting ground was implemented in the FDTD model. The experimental results of a wind tunnel study, set up to improve noise barrier performance in wind with the use of windscreens, were simulated with the described model. Windscreens reduce the screen-induced refraction of sound efficiently. High-detailed CFD calculations in the vicinity of the noise barriers were used to obtain the background flow for the acoustic calculations. Good agreement between experimental and measured net efficiency of the windscreens was obtained. Turbulent effects, not considered in this paper, could improve this agreement, especially for the cases where wind shielding is limited.

REFERENCES

- [1] R. DeJong, E. Stusnick, "Scale model studies of the effect of wind on acoustic barrier performance", *Noise control engineering* **6** (1976), p. 101-109.
- [2] E.M. Salomons, "Reduction of the performance of a noise screen due to screen-induced wind-speed gradients. Numerical computations and wind tunnel experiments", *J. Acoust. Soc. Am.* **105** (1999), p. 2287-2293.
- [3] T. Van Renterghem, D. Botteldooren, "Reducing screen-induced refraction of noise barriers in wind by vegetative screens", *Acustica – acta acustica* **88** (2002), p. 231-238.
- [4] D. Botteldooren, "Finite-difference time-domain simulation of low-frequency room acoustic problems", *Journal of the Acoustical Society of America* **98** (1995), p. 3302-3308.
- [5] D. Botteldooren, "Acoustical finite-difference time-domain simulations in a quasi-Cartesian grid", *Journal of the Acoustical Society of America* **95** (1994), p. 2313-2319.
- [6] C. Zwikker, C.W. Kosten, *Sound absorbing materials*, Elsevier, New York, 1949.
- [7] J.P. Berenger, "A Perfectly matched layer for the absorption of electromagnetic waves", *Journal of Computational Physics* **114** (1994), p. 185-200.
- [8] J.P. Berenger, "Perfectly matched layer for the FDTD solution of wavestructure interaction problems", *IEEE Antennas Propagation Symposium* **44** (1996), p. 110-117.
- [9] STAR-CD (version 3.100A), Computational dynamics LTD, London, 2000.
- [10] W. Dierickx, "Flow reduction of synthetic screens obtained with both a water and airflow apparatus", *J. Agric. Eng. Res.* **71** (1998), p. 67-73.